GEOMETRICAL FACTORS INFLUENCING MUSCLE FORCE DEVELOPMENT

I. The Effect of Filament Spacing upon Axial Forces

MARK SCHOENBERG, *Laboratory of Physical Biology, National Institute of Arthritis, Metabolism, and Digestive Diseases, National Institutes of Health, Bethesda, Maryland 20205 U.S.A.*

ABSTRACT The influence of geometry on the force and stiffness measured during muscle contraction at different sarcomere lengths is examined by using three specific models of muscle cross-bridge geometry which are based upon the double-hinge model of H. E. Huxley (*Science* [*Wash. D.C.*], 1969, **164**:1356–1366) extended to three dimensions. The force generated during muscle contraction depends upon the orientation of the individual cross-bridge force vectors and the distribution of the cross-bridges between various states. For the simplest models, in which filament separation has no effect upon cross-bridge distribution, it is shown that changes in force vectors accompanying changes in myofilament separation between sarcomere lengths 2.0 and 3.65 μm in an intact frog skeletal muscle fiber have only a small effect upon axial force. The simplest models, therefore, produce a total axial force proportional to the overlap between the actin and myosin filaments and independent of filament separation. However, the analysis shows that it is possible to find assumptions that produce a cross-bridge model in which the axial force is not independent of filament spacing. It is also shown that for some modes of attachment of subfragment-1 (S1) to actin the azimuthal location of the actin site is important in determining the axial force. A mode of S1 attachment to actin similar to that deduced by Moore et al. (*J. Mol. Biol.*, 1970, **50**:279–294), however, exhibits rather constant cross-bridge behavior over a wide range of actin site location.

INTRODUCTION

Using a spot follower device to keep a portion of a frog skeletal muscle fiber at constant length, Gordon et al. (1966) concluded that the force a muscle produced at sarcomere lengths between 2 and 3.6 μm was proportional to the amount of overlap between the cross-bridge region of the myosin and the actin filament. Since the distance between the actin and myosin filaments in a contracting intact frog fiber varies as sarcomere length is changed (Elliott et al., 1967), these findings suggest that either the force of each cross-bridge is independent of filament separation or that the entire ensemble of cross-bridges produces a force that is on the average independent of filament separation (Hill, 1970). H. E. Huxley pointed out that if the cross-bridge was flexible near the region of the myosin subfragment-1 (S1)-subfragment-2 (S2) junction and also the S2-light meromyosin (LMM) junction, then the S1 "head" region of the myosin could interact with the actin filament at constant orientation, regardless of filament separation (Huxley, 1969; Lowey et al., 1969; Mendelson et al., 1973; Burke et al., 1973; Elliott and Offer, 1978). T. L. Hill (1970) showed mathematically that for certain values of a parameter characterizing the cross-bridge compliance a cross-bridge model of the

kind proposed by H. E. Huxley would produce a somewhat increased force at increased filament separation, while for others it would produce a somewhat decreased force over the same range of spacing. This suggested that for a suitable intermediate parameter value the force per cross-bridge could be approximately independent of filament spacing.

Recently, experimental findings of ter Keurs et al. (1978), who remeasured the length-tension relationship of intact skeletal muscle fibers, and Godt and Maughan (1977), who measured the calcium-activated force of osmotically compressed skinned muscle fibers, have suggested that the axial force per cross-bridge might not be independent of filament spacing. For this reason, this paper examines in detail the equations governing the behavior of a cross-bridge, paying particular attention to the geometrical factors that influence muscle force development at different filament separations. The approach was to consider three rather simple models of the cross-bridge under a reasonable set of assumptions, to see if these models produced constant axial force at different filament separation. The conclusion is that these "simplest" models do produce very nearly constant axial force over the physiological range of filament spacings. However, the analysis also shows that it is possible to find assumptions that produce cross-bridge models in which the axial force is not independent of filament spacing.

METHODS

Geometry

Most previous models of cross-bridge action have assumed that the actin filament, myosin filament, and S1 "head" portion of the myosin all lie in the same plane. Recent work using polarization anisotropy decay and electron-microscopic evidence (Moore et al., 1970; Mendelson et al., 1973; Elliott and Offer, 1978) suggests that the S1 head is larger than the surface-to-surface distance between actin and myosin filaments, particularly at long sarcomere length, so that the S1 "head" probably does not lie in the same plane as the actin and myosin filaments. A detailed description of the three-dimensional geometry of the actin and myosin filaments and the cross-bridges may be found in the review by Squire (1975). Fig. 1 illustrates the three-dimensional aspects we are concerned with and also the important variables. The subfragment-2 portion of the cross-bridge, S2, is considered elastic, having a length, ℓ_2, which is equal to ℓ_2^o when unstressed. Fig. 2 illustrates several of the possible modes of attachment of the cross-bridge head, S1, to an actin site and illustrates the definition of the variable, γ. The cross-bridge head may attach with its long axis pointing through the center of the actin filament, as in Fig. 2 *a* ($\gamma = 0$), or it may attach slewed, as in Figs. 2 *b* and *c*. Both the actin attachment sites and the cross-bridge origin sites are known to be distributed at different azimuthal angles with respect to the filaments, and their azimuthal locations may be defined in terms of the azimuthal angle they make with the plane of the axes of the actin and myosin filaments (ϕ and θ, respectively, in Fig. 1 *B*).

Each myosin molecule has two S1 heads per S2. In the analyses that follow, the complications that arise from consideration of both heads binding to sites on the same or different actin filaments have not been considered. (For further discussion, see Hill, 1975, pp. 128–132.)

For computation, ℓ_1, the length of S1, was taken as 16 nm, while ℓ_2^o was taken as 40 nm. These values are not too different from those reported by Mendelson et al. (1973) and Elliott and Offer (1978). The diameters of the filaments were 8 nm for actin and 14 nm for myosin, resulting in a surface-to-surface separation of 13 nm at a sarcomere length of 2.1 μm (Huxley, 1963; Huxley and Brown, 1967). The myofilament lattice during contraction was assumed to follow a constant volume relationship as sarcomere length varied (Elliott et al., 1967), so that the surface-to-surface separation of the actin and myosin filaments was only 7.9 nm at 3.4 μm.

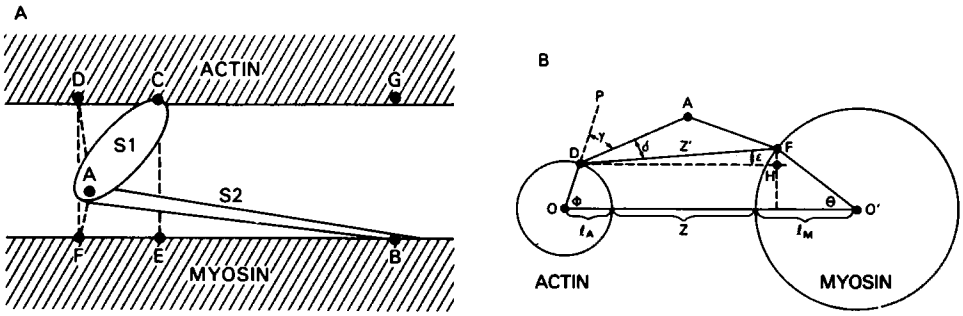

FIGURE 1 (*A*) One possible arrangement of a muscle cross-bridge in three dimensions, drawn approximately to scale at a filament separation appropriate to a sarcomere length of 2.1 μm (axial view). Note that point *A* need not lie in the same plane as the filaments. *DCG* is a line through the actin attachment site, *C*, parallel to the actin filament axis, and *FEB* is a line through the cross-bridge origin site, *B*, parallel to the myosin filament axis. The length of the S1 "head" portion of the cross-bridge, ℓ_1, is equal to $\overline{AC}$. $\ell_2 = \overline{AB}$ is the length of the S2 portion of the cross-bridge, linking the "head" at *A* with the myosin filament at *B*. *CE* is a perpendicular from point *C* to *FEB*, *AF* is a perpendicular from the S1–S2 junction to this same line, and *AD* is a perpendicular to *DCG*, as is *BG*. Since the filaments are parallel, *DCG* is parallel to line *FEB*, so that *DF* is parallel to *CE*. $\overline{EB}$ is defined as x, the distance between the origin of the cross-bridge, *B*, and the longitudinal position of the actin site, *C*.

(*B*) Cross-sectional view through the actin and myosin filaments. *O* and *O'* connote the centers (axes) of the actin and myosin filaments, respectively. Point *A* is the S1–S2 junction. In this view, the S1 head, *AC*, is projected along *AD*, and the actin site, *C*, is projected into point *D*. The S2 portion of the cross-bridge, *AB*, is projected along *AF* with point *B* projected into *F*. The surface-to-surface separation of the filaments is *Z*, and the radii of the actin and myosin filaments, ℓ_A and ℓ_M, respectively. The angle defining the azimuthal location of the actin site is ϕ; that defining the origin of the S2 on the myosin is θ. The azimuthal angle that defines the orientation of an attached cross-bridge head with respect to a normal to the actin surface is γ. Other parameters used in the equations include $\epsilon = \angle FDH$, and $Z' = \overline{DF}$.

Mechanism of Force Generation

In our discussion we restrict ourselves solely to "sliding filament" models of muscle contraction in which force is produced after physical contact between the actin and the S1 head. We assume, as did Hill (1970), that when the S1 head attaches to actin it does so at an axial tilt angle near its equilibrium axial attachment angle, $\alpha^* = \alpha_0$. (The angle α is $\angle ACD$ in Fig. 1). We further assume that subsequently there

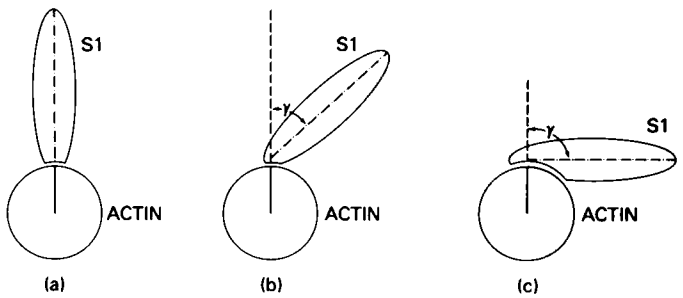

FIGURE 2 Three modes of attachment of S1 to actin. In *a*, $\gamma = 0°$ and the long axis of the S1 projects through the actin filament axis. In *b* and *c*, the cross-bridge is slewed, i.e., $\gamma \neq 0$. In *c*, $\gamma = 90°$ and the long axis of the S1 is actually parallel to a tangent at the site of attachment.

is a change of state such that a new equilibrium angle $\alpha^* = \alpha_1$, $\alpha_1 < \alpha_0$, is preferred. A torque is thereby generated about point C which tends to bring the cross-bridge toward $\alpha = \alpha_1$. This torque has a component of force that is transmitted to the myosin filament through the S2 connection, which tends to produce shortening. It seems reasonable to assume that the torque generated by the reaction of the cross-bridge at site C is independent of filament separation. Even with this assumption (which we use here), the axial component of the generated force, (that measured by a force transducer attached to the end of the fiber), will generally not be independent of filament spacing, since its magnitude will depend upon $\angle ABF$ in Fig. 1.

Axial Tilt Angles ($\alpha \equiv \angle ACD$, Fig. 1 A)

The choice of axial tilt angles, α_0 and α_1, is somewhat arbitrary, since little is definitively known about the angles of attachment during the cross-bridge cycle. α_1 was taken as 45° because this seems to be the preferred orientation of the cross-bridge in rigor (Reedy et al., 1965; Reedy, 1967; Moore et al., 1970). $\alpha_0 = 90°$ was chosen because the cross-bridges in relaxed insect muscle seem to project at ~90° (Reedy et al., 1965) and in the same preparation there is the suggestion that an attached nonforce-producing cross-bridge with β, γ-imido-adenosine triphosphate (AMP-PNP) bound exists at an angle nearer to 90° than 45° (Goody et al., 1975; Marston et al., 1976, 1979). These are not very strong reasons for the choice of α_0, since cross-bridges in other muscles at rest are known to have other configurations (Wray et al., 1975), but the exact choice of α_0 and α_1 is not critical for the questions addressed.

Azimuthal Location of the Actin Sites (ϕ, Fig. 1 B)

It appears likely that cross-bridges attach to actin sites located at a variety of azimuthal angles with respect to the plane of the axes of the filaments (Squire, 1972; Haselgrove and Reedy, 1978). The reason for supposing this is that the axial and azimuthal periodicity of the actin helix is different from that of the myosin. If there were not some latitude (flexibility) in the ability of the cross-bridge to attach to sites at different axial and azimuthal positions, very few cross-bridges would find themselves in the proper position to attach. This was the argument of Squire (1972) and Haselgrove and Reedy (1978), who suggested that about two-thirds of the cross-bridges can attach to actin sites when the range of azimuthal location of sites allowing attachment is ~90°. Each of the models considered here was explored over a range of azimuthal angles of at least 120°.

Azimuthal Orientation (Slew) of the Cross-Bridge (γ, Fig. 2)

For ease of calculation the assumption was made that once a cross-bridge attaches, subsequent changes in state or axial tilt angle, α, do not include a change in azimuthal orientation of the S1 head, although this would not have to be the case.

Flexibility of the Hinge Regions (Points A and B, Fig. 1)

The S1-S2 hinge region, point A in Fig. 1, was assumed to behave as a universal joint, in line with the conclusions of Mendelson et al. (1973) from polarization anisotropy decay measurements. The S2-LMM junction, point B in Fig. 1, was also assumed to behave as a universal joint, although there is very meager evidence concerning this assumption (Burke et al., 1973; Elliott and Offer, 1978).

Three Specific Models

Doing mechanical quick-release experiments, Ford et al. (1978) showed that frog skeletal muscle has a compliance of some 5 nm/half-sarcomere for zero to full isometric tension. The three basic models we will consider differ in the location of this compliance. In Model I, the compliance resides in the S2 link between the head and the myosin backbone, the same location as in the example given by Huxley and Simmons (1971). In Model II, the elasticity resides in the rotation of the S1 head (change of α), as in

Eisenberg and Hill (1978). For Model III, the compliance is within the myosin filament itself, as would be the case if the backbone (LMM) part of each myosin molecule were not completely constrained from longitudinal movement within the myosin filament.

MODEL I In Model I, the cross-bridge compliance resides in the S2 link. In this case, when the cross-bridge changes state, it rotates to the equilibrium angle, α_i^*, for that state. The energy is stored in the stretched-out S2 link. The configurations the cross-bridge attains in this model are then identical to those attained by the cross-bridges in the Huxley and Simmons (1971) example, as they "fall" into their various energy wells. This is true even though the mechanism driving the angle change is fundamentally different (Hill [1974] pp. 311–320) in the two cases. In both cases, as the filaments are moved relative to each other with no change of cross-bridge angle, the force changes as the S2 link is either released or stretched.

MODEL II For Model II, the compliance is not in the S2 link but resides in the angular configuration of the cross-bridge, as in the model of Eisenberg and Hill (1978). In their model, when the cross-bridge changes state without relative filament movement, there is no cross-bridge motion. However, force is generated because the change in state signifies a change in equilibrium angle, so that even though no actual cross-bridge movement occurs, the cross-bridge is now further from its equilibrium position. When the filaments do move past each other, the force varies depending upon whether the cross-bridge angle moves further or closer from its equilibrium position.

MODEL III In this model, the cross-bridge compliance resides in the link of the S2 to the myosin filament backbone, with the origin of the S2 link from the backbone shifting somewhat as force is exerted. This differs from the other two models in that the direction of the compliance extension is along the same direction as the measured force, i.e., axial.

Each of the models was computed for two cases, $\gamma = 0°$ and $\gamma = 90°$ (Figs. 2 *a* and *c*). The figures and tables show $\gamma = 0°$. The case $\gamma = 90°$ is considered in the Discussion. Although the figures and tables show computations for cross-bridges originating from the myosin at an azimuthal angle of 0°, additional computation revealed the conclusions to be generally true for cross-bridge origins between $0 < \theta < 60°$.

Equations

The equations governing the behavior of the cross-bridge may be derived as follows. For our models, the cross-bridge is assumed to be at its lowest energy when the S1 head makes an angle, $\alpha = \alpha^*$, with the actin filament; when it is not at this preferred angle, a torque exists driving it towards this angle. This is our assumed force-generating mechanism. At steady state, the torque generated by the interaction at point *C*, Fig. 1, must just be balanced by the torque (about point *C*) generated by the force in *AB*. In the simplest (linear) case this first torque is proportional to the deviation of the cross-bridge angle from its equilibrium value so that we may write

$$\tau_A = \Gamma \ell_1^2 (\alpha - \alpha^*), \tag{1}$$

where $\Gamma \ell_1^2$ is the constant of proportionality.

If the S2 link, *AB*, has a linear stiffness denoted by *K*, then the force along *AB* is

$$F = K(\ell_2 - \ell_2^\circ), \tag{2}$$

where ℓ_2° is the unstrained length of S2 and ℓ_2 the strained length.

The balancing torque, τ_B, exerted by the force, *F*, may be found from the geometry by calculating the component of the force, *F*, in plane *ACD* (the plane in which τ_A is acting). This is done in Appendix II. Setting $\tau_A = \tau_B$, we have, from Eq. A2.1,

$$\tau_A = \tau_B = F \cdot \ell_1 \cdot (x \sin \alpha + Z' \cos \delta \cos \alpha)/\ell_2. \tag{3}$$

The geometric variables are defined in Fig. 1. ℓ_2 in Eqs. 2 and 3 is related to these geometric variables according to the relationship

$$\ell_2 = [Z'^2 + \ell_1^2 + x^2 + 2\ell_1(x \cos \alpha - Z' \cos \delta \sin \alpha)]^{1/2}. \quad (4)$$

(See Appendix III for derivation.)

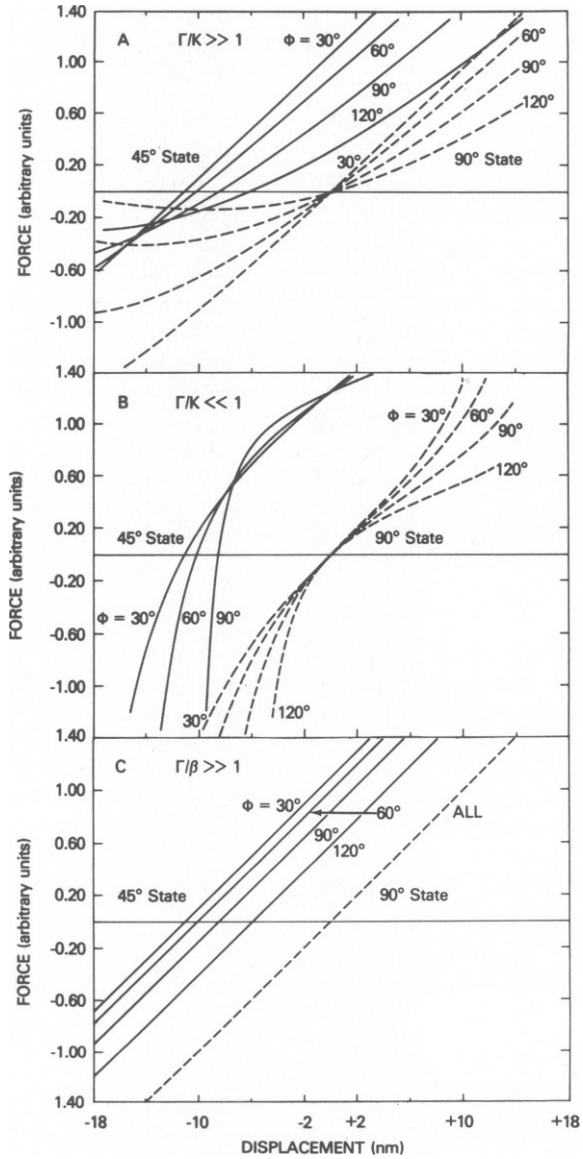

FIGURE 3 Typical force-displacement relationships for the three cross-bridge models. (*A*) Model I, $\Gamma/K \gg 1$. (*B*) Model II, $\Gamma/K \ll 1$. (*C*) Model III, $\Gamma/\beta \gg 1$. Curves are shown for the 90° "state" (dashed lines) and the 45° "state" (solid lines), for actin site azimuthal angles of ϕ = 30, 60, 90, and 120°. For each case, filament separation, Z = 15 nm and γ = 0°.

Given the actin site azimuthal location, ϕ, the filament separation, Z, and the relative axial position of the cross-bridge, x, simultaneous solution of Eqs. 1–4, allows computation of the steady-state values of axial tilt angle, α, and ℓ_2 for any cross-bridge state, each state being characterized by its equilibrium angle, α^*. (The relationship between δ and Z' used in the equations, and ϕ and Z, the more common variables referred to in the tables, is shown in Appendix I.)

Once α and ℓ_2 are known, the axial force component, f_x, the force that would be recorded by a transducer attached to one end of the muscle, may be calculated as: $f_x = F \cos \angle ABF = K(\ell_2 - \ell_2^o) \cdot \overline{FB}/\ell_2$, or, using Eq. A3.2,

$$f_x = K(\ell_2 - \ell_2^o)(x + \ell_1 \cos \alpha)/\ell_2. \tag{5}$$

For Model III, where the compliance resides in the site of origin of the cross-bridge and is along the myosin filament, we may write in place of Eq. 5

$$f_x = \beta(x - x_r), \tag{6}$$

where β is the stiffness with which the origin of the cross-bridge is held in place within the myosin filament, and x_r is a reference location. For convenience, x_r is selected so that the force is zero when $x = x_r$, $\ell_2 = \ell_2^o$, and $\alpha = 90°$. From Eq. 4,

$$x_r = (\ell_2^{o2} - Z'^2 - \ell_1^2 + 2\ell_1 Z' \cos \delta)^{1/2}. \tag{7}$$

Solution of the Equations

Eqs. 1–5 or 6 are nonlinear algebraic equations which may be solved using the Newton-Raphson iterative procedure. With appropriate initial estimates, a solution for α, ℓ_2, and f_x could usually be found to accuracy greater than one part in 1,000 in fewer than 10 iterations. The equations apply to all three models. For Model I, we set $\Gamma/K \gg 1$, for Model II, $\Gamma/K \ll 1$, and for Model III, $\Gamma/\beta \gg 1$.

RESULTS

In this section we will concentrate upon elucidating which parameters influence the ability of a cross-bridge to produce force at different filament separations. With regard to this question, the three models behave similarly, even though they differ widely in the location of the cross-bridge compliance.

TABLE I
AXIAL FORCE (f_x) AND DISPLACEMENT NECESSARY TO REDUCE FORCE TO ZERO ($\Delta x_{f=0}$) FOR MODEL I, $\Gamma/K \gg 1$

	ϕ = 30°		ϕ = 60°		ϕ = 90°		ϕ = 120°	
	f_x	$\Delta x_{f=0}$	f_x	$\Delta x_{f=0}$	f_x	$\Delta x_{f=0}$	f_x	$\Delta x_{f=0}$
	(arbitrary units)	*(nm)*	*(arbitrary units)*	*(nm)*	*(arbitrary units)*	*(nm)*	*(arbitrary units)*	*(nm)*
Z = 5 nm	100	(10.1)	91	(9.6)	78	(8.9)	64	(8.1)
Z = 10 nm	106	(10.6)	92	(9.9)	71	(8.8)	50	(7.3)
Z = 15 nm	109	(11.1)	90	(10.2)	62	(8.6)	33	(6.0)
Z = 20 nm	110	(11.7)	86	(10.5)	49	(8.2)	8	(2.8)

ϕ is the azimuthal angle of the actin site and Z is the surface-to-surface filament separation. Model values are γ = 0°, θ = 0°, and $x' = x - x_r = 0$. S1 = 16 nm, S2 = 40 nm.

TABLE II

AXIAL FORCE (f_x) AND DISPLACEMENT NECESSARY TO REDUCE FORCE TO ZERO ($\Delta x_{f=0}$) FOR MODEL II, $\Gamma/K \ll 1$

	ϕ = 30°		ϕ = 60°		ϕ = 90°		ϕ = 120°	
	f_x	$\Delta x_{f=0}$	f_x	$\Delta x_{f=0}$	f_x	$\Delta x_{f=0}$	f_x	$\Delta x_{f=0}$
	(arbitrary units)	*(nm)*	*(arbitrary units)*	*(nm)*	*(arbitrary units)*	*(nm)*	*(arbitrary units)*	*(nm)*
Z = 5 nm	100	(10.1)	100	(9.6)	100	(8.9)	100	(8.1)
Z = 10 nm	100	(10.6)	100	(9.9)	100	(8.8)	100	(7.3)
Z = 15 nm	100	(11.1)	100	(10.2)	100	(8.6)	100	(6.0)
Z = 20 nm	100	(11.7)	100	(10.5)	100	(8.2)	100	(2.8)

ϕ is the azimuthal angle of the actin site and Z is the surface-to-surface filament separation. Model values are γ = 0°, θ = 0°, and $x' = x - x_r = 0$. S1 = 16 nm, S2 = 40 nm.

Force-Displacement Relationships

For a given cross-bridge geometry and state, the relationship between the force the cross-bridge exerts and the relative axial position of the filaments (x or $\overline{EB}$ in Fig. 1 *A*) may be derived from the equations of the previous section. Typical curves are shown in Fig. 3. The linearity of each curve correlates directly with how well the cross-bridge compliance maintains its orientation relative to the x-axis. In Model III (Fig. 3 *C*), where the compliance (assumed linear) always lies along the x-direction, the force-displacement curves are perfectly linear. For Model I (Fig. 3 *A*), where the compliant S2 for the most part lies approximately along the x-axis (due to its long length, as discussed later), the curves are mostly linear.

The force-displacement relationship of a cross-bridge contains much information regarding its behavior. For example, at an actin site located at an azimuthal angle of 30°, the axial force generated by a cross-bridge attaching in the "90° state" and then transforming to the "45° state" may be determined from the vertical separation of the 30° curves of the two states. Likewise, a measure of the compliance of that cross-bridge is the distance the filaments need to move relative to each other to reduce the generated force to zero. This is measured by the horizontal separation of the two curves.

These two parameters, f_x and $\Delta x_{f=0}$, respectively, are summarized in Tables I, II, and III

TABLE III

AXIAL FORCE (f_x) AND DISPLACEMENT NECESSARY TO REDUCE FORCE TO ZERO ($\Delta x_{f=0}$) FOR MODEL III, $\Gamma/\beta \gg 1$

	ϕ = 30°		ϕ = 60°		ϕ = 90°		ϕ = 120°	
	f_x	$\Delta x_{f=0}$	f_x	$\Delta x_{f=0}$	f_x	$\Delta x_{f=0}$	f_x	$\Delta x_{f=0}$
	(arbitrary units)	*(nm)*	*(arbitrary units)*	*(nm)*	*(arbitrary units)*	*(nm)*	*(arbitrary units)*	*(nm)*
Z = 5 nm	100	(10.1)	95	(9.6)	88	(8.9)	80	(8.1)
Z = 10 nm	105	(10.6)	98	(9.9)	87	(8.8)	72	(7.3)
Z = 15 nm	110	(11.1)	101	(10.2)	85	(8.6)	59	(6.0)
Z = 20 nm	116	(11.7)	104	(10.5)	81	(8.2)	28	(2.8)

ϕ is the azimuthal angle of the actin site and Z is the surface-to-surface filament separation. Model values are γ = 0°, θ = 0°, and $x' = x - x_r = 0$. S1 = 16 nm, S2 = 40 nm.

for each of the models considered for a variety of filament separations and actin site azimuthal locations. It can be seen that for these models: (*a*) cross-bridges at actin sites located at different azimuthal angles behave differently; (*b*) cross-bridges at actin sites located azimuthally quite distant, i.e., $\phi = 120°$, show fairly large variation in behavior with filament separation; and (*c*) curiously, the azimuthal actin site location that minimizes the deviation of f_x with filament separation (~60°) is different from the location (just under 90°) that

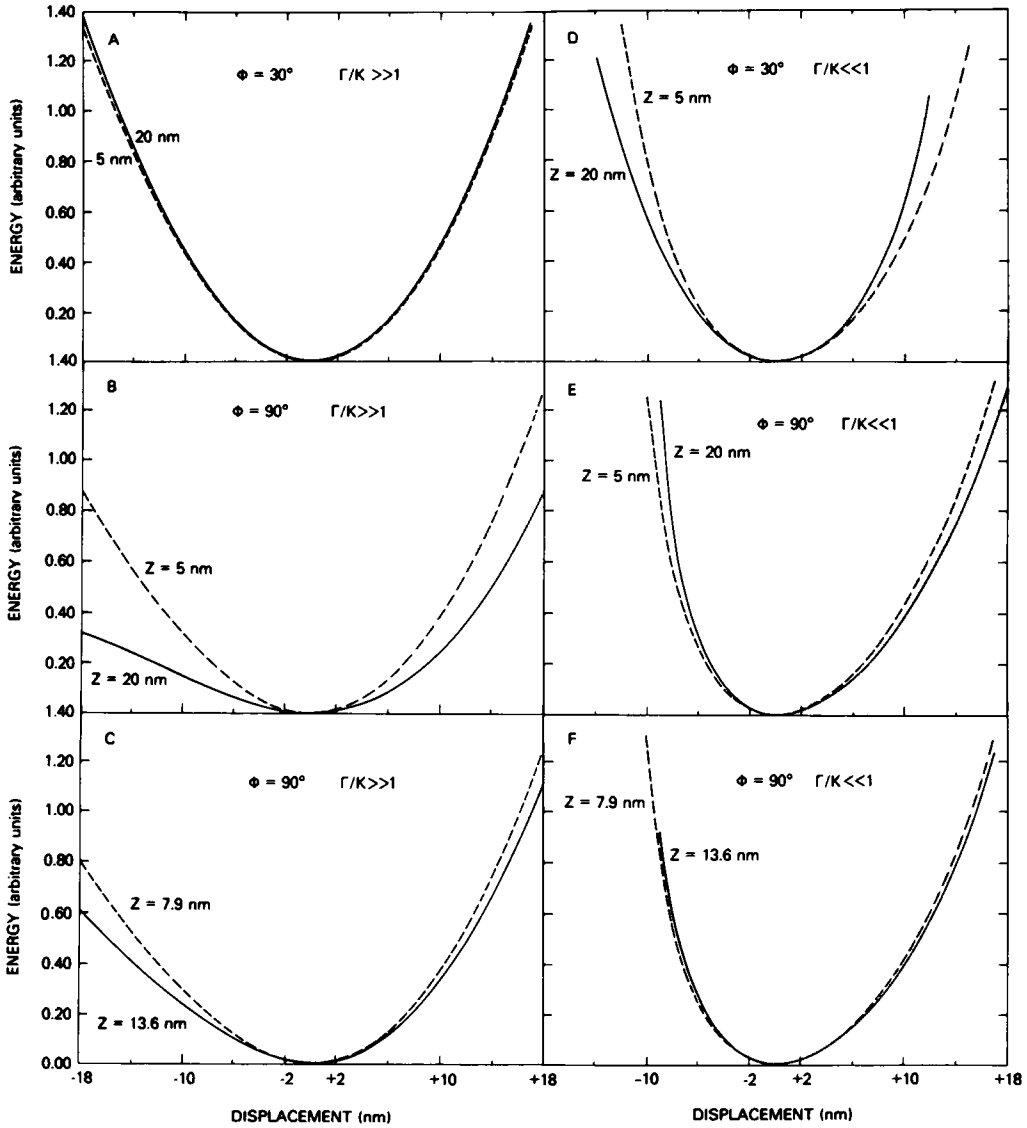

FIGURE 4 Free energy diagrams for the 90° state ($\alpha^* = 90°$) for Model I, $\Gamma/K \gg 1$ (*A-C*) and for Model II, $\Gamma/K \ll 1$ (*D-F*). Values of site azimuthal angle, ϕ, and filament spacing, Z, accompany each diagram. The curve for the smaller filament separation in each case is shown dashed. *C* and *F* show the range of free energy diagrams for filament separations existing in an intact fiber between sarcomere lengths 2.0 and 3.4 μm. The vertical level of each curve is, in general, different and not zero, as illustrated here for clarity.

minimizes the variation in distance to zero force ($\Delta x_{f=0}$) with filament separation. The significance of these results and their generality for other models is discussed later.

Constancy of Force per Cross-Bridge for Model II ($\Gamma/K \ll 1$)

Table II reveals that for Model II the axial cross-bridge force is independent of filament spacing and azimuthal location of the actin site. Here we show that this result is not a general property of models having $\Gamma/K \ll 1$, but is exactly true only when $\alpha_0 \equiv 90°$.

From Eqs. 1–3, $\tau_A = \tau_B = K(1 - \ell_2^o/\ell_2) \cdot \ell_1 \cdot (x \sin \alpha + Z' \cos \delta \cos \alpha)$, and Eq. 5 is $f_x = K(\ell_2 - \ell_2^o)(x + \ell_1 \cos \alpha)/\ell_2$, so that

$$f_x = (\tau_A/\ell_1) \cdot (x + \ell_1 \cos \alpha)/(x \sin \alpha + Z' \cos \delta \cos \alpha)$$

$$_x = \Gamma\ell_1(\alpha - \alpha^*) \cdot (x + \ell_1 \cos \alpha)/(x \sin \alpha + Z' \cos \delta \cos \alpha). \quad (8)$$

From Eq. 8 it is seen that if $\alpha \equiv 90°$, then f_x is independent of Z' and δ, or alternatively, Z and ϕ. This agrees with the findings of Hill (1970) for the two-dimensional case. The constancy of force per cross-bridge, shown in Table II, results therefore because the force is calculated for a cross-bridge attaching at 90°, remaining there even when α^* goes to 45°. (As stated previously, when K is $\gg \Gamma$, the cross-bridge is unable to rotate unless there is filament movement.) If the initial attachment were at an angle other 90°, or if K were not $\gg \Gamma$, the force generated by the change of state in Model II would depend upon filament separation and site azimuthal angle, as in the other examples considered.

Free Energy Diagrams

Hill (1974, 1975) has shown it is useful to describe a given cross-bridge state in terms of how its free energy varies with x. This information can be obtained directly from the force-displacement relationships, since the force is equal to the derivative of the basic free energy with respect to x or, conversely, the free energy change with x is simply the integral of the force-displacement relationship. Alternatively, for each model, the free energy stored in a cross-bridge at a given x value may be calculated directly. For Model I, the free energy is stored in the S2 link and its value is $0.5\ K(\ell_2 - \ell_2^o)^2$. When $\Gamma/K \gg 1$, as in Model II, the free energy is stored in the displacement of the head from its equilibrium angle and is equal to $0.5\ \Gamma\ell_1^2\ (\alpha - \alpha^*)$.[2] For Model III, $\Gamma/\beta \gg 1$, the stored free energy is simply $0.5\ \beta(x - x_r)$.[2] For Model I, ℓ_2 is a function of α, x, ϕ, and Z, as per Eq. 4.

Fig. 4 shows the free energy diagrams derived from Fig. 3 for the "90° state" ($\alpha^* = 90°$) for Models I and II and for several different site azimuthal angles (ϕ) and filament separations (Z). Although in each case the shape of the free energy diagram versus x for a given attached state changes with filament spacing, over the range of filament spacings encountered in an

---

FIGURE 5 The effect of changes in orientation of the force vectors with sarcomere length upon the length versus tension or stiffness relationships. (*A*) Model I, $\Gamma/K \gg 1$. (*B*) Model II, $\Gamma/K \ll 1$. (*C*) Model III, $\Gamma/\beta \gg 1$. (●), axial force; (○), axial stiffness. Left-most curves, $\phi = 90°$. Right-most curves, $\phi = 120°$. Computed for a homogeneous population of cross-bridges attaching in the 90° state at zero force ($x' = 0$) and then transforming to the 45° state. The solid line, from Gordon et al. (1966), is the hypothetical force or stiffness versus sarcomere length when the force or stiffness per cross-bridge is independent of filament spacing. Azimuthal angles smaller than those depicted show lesser deviations. These curves do not include possible effects of filament separation upon cross-bridge distribution.

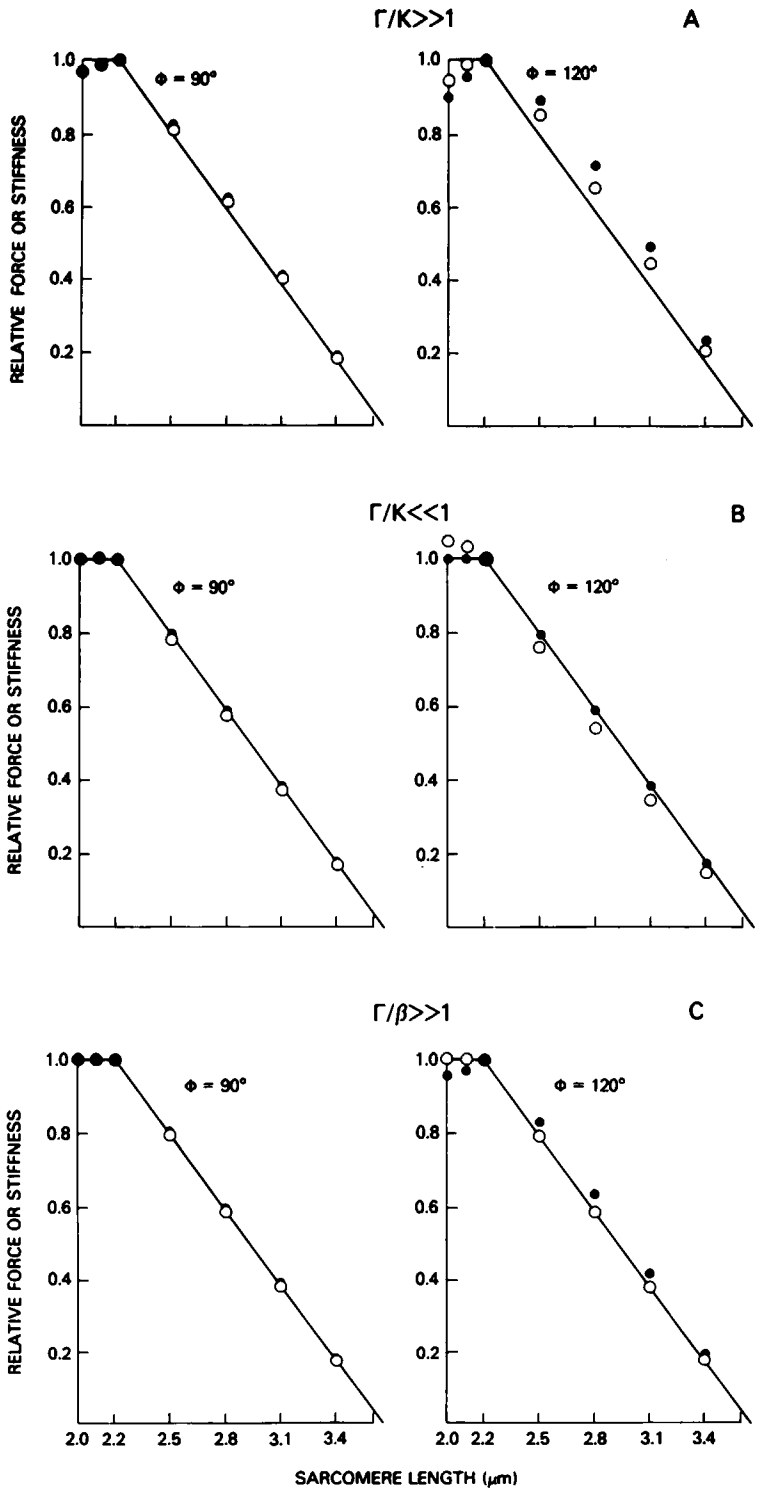
Γ/K>>1
A
Φ = 90°
Φ = 120°
RELATIVE FORCE OR STIFFNESS
1.0
0.8
0.6
0.4
0.2
Γ/K<<1
B
Φ = 90°
Φ = 120°
RELATIVE FORCE OR STIFFNESS
Γ/β>>1
C
Φ = 90°
Φ = 120°
RELATIVE FORCE OR STIFFNESS
2.0 2.2 2.5 2.8 3.1 3.4
SARCOMERE LENGTH (μm)

intact frog fiber between sarcomere lengths 2.0 and 3.4 μm (Figs. 4 *C* and *F*), the changes with filament spacing for ϕ between 30 and 90° are small for Model II and not very great for Model I. For $\phi = 120°$ (not shown) the changes begin to be significant in both models. Model III (not illustrated) has the special property that the cross-bridge compliance lies along the x-axis. For this type of model, the free energy variation with x is independent of either filament separation or actin site location (ϕ). The significance of these results is discussed later.

Axial Force and Stiffness as a Function of Sarcomere Length

One of the fundamental questions concerning cross-bridges is whether they can produce relatively constant force per unit of overlap between the cross-bridge region of the myosin and the actin filament for sarcomere lengths between 2.0 and 3.65 μm, even though the filament separation changes from 13.6 to 7.2 nm over this range. Filament spacing changes associated with sarcomere length changes could affect (*a*) the individual force-displacement relationships and (*b*) the specific distribution of the cross-bridges.

We can get an idea of the order of magnitude of the first of these factors by examining a homogeneous population of cross-bridges. For example, Fig. 5 shows for each of the models the variation in force and stiffness with sarcomere length expected from a homogeneous population of cross-bridges attaching in the 90° state at zero force ($x' = 0$ and then transforming to the 45° state. The deviation from constancy of force and stiffness per length of overlap (i.e., from the solid line in Fig. 5) is hardly noticeable for $\phi < 90°$ and just barely noticeable for $\phi = 120°$. The significance of this finding is considered in the Discussion.

DISCUSSION

The length-tension diagrams obtained by Gordon et al. (1966) suggest that the average force exerted per cross-bridge is independent of filament spacing. However, those of ter Keurs et al. (1978) do not. Also, Godt and Maughan (1977) measured a 20–30% decrease in active axial force when a skinned fiber (initially swollen) was compressed ~30% using either polyvinylpyrrolidone (PVP) or dextran T40 in the bathing solution. Goldman and Simmons (1978) reported a 100% increase in stiffness from the same maneuver. It is therefore useful to consider what types of cross-bridge models predict nearly constant force at varying filament separation and what types do not.

Filament spacing change can affect force by affecting the distribution of cross-bridges (by changing rate constants of transition between states) or it can have a direct effect upon each cross-bridge by changing the orientation of the individual force vectors. Fig. 5 suggests that for each of the models detailed here this latter effect is moderately small. In fact, the overall effect would likely be even smaller than suggested by Fig. 5 for two reasons. First, in Fig. 5 the largest effect of filament spacing upon force is seen for $\phi = 120°$, $\Gamma/K \gg 1$. However, the force (Table I) from cross-bridges attached at the site $\phi = 120°$ is smaller than that from other locations, so that changes in it have proportionally less effect overall. Second, for reasons discussed earlier, cross-bridges probably exist over a range of azimuthal angles and, as seen from the tables, force increases with increasing filament spacing for some azimuthal angles while for others it decreases. Therefore, for all the cross-bridges averaged, the overall change in axial force with filament spacing would be small. The same arguments apply to

cross-bridge compliance (or stiffness), suggesting that these properties are also insensitive to filament spacing for the models considered here.

One reason these models show very little change in axial force or stiffness with filament separation is the long length of S2 relative to the interfilament distance, as suggested by Huxley (1969). For any model, as the length of S2 becomes large, the influence of changes in the force vectors associated with changes in filament spacing approaches zero. However, if the S2 portion of the myosin molecule were not free to swing away from the myosin filament, if it were constrained for some reason to stay near the myosin backbone, as suggested by Sutoh et al. (1978), then this type of cross-bridge would be much less likely to behave similarly at different filament spacings.

The effect of filament separation upon cross-bridge distribution depends upon the effect of filament spacing on the individual rate constants for transitions between states. That the shape of the free-energy curves of Figs. 5 *C* and *F* is relatively independent of filament spacing suggests that it is allowable for the rate constants also to be relatively independent of filament spacing (Hill, 1974, 1975). This, in turn, would make the distribution of cross-bridges independent of spacing. However, as Hill points out, although the similarity of shape of the various free energy curves places restraints upon the ratio of certain rate constants, the individual rate constants could be quite sensitive to filament spacing. For a system with more than two states, in steady state as opposed to equilibrium, it is the individual rate constants and not their ratios that are important in determining distribution. Clearly, if the cross-bridge distribution were sensitive to filament spacing, the net force output at different filament separations could also vary. Unfortunately, very little is now known about the behavior of the individual rate constants with geometry. In the model of Huxley and Simmons (1971), the rate constants for transition between the attached states were assumed related to the strain in the elastic element. In the model of Eisenberg and Hill (1978), the dependence of the rate constants upon geometry (other than their x-dependence) was not discussed.

Another factor potentially affecting the force output of a muscle is the possible effect of filament spacing upon the azimuthal distribution of cross-bridges. Any factor that could change the angular distribution of site locations allowing cross-bridge attachment might also change the overall force or even the force or stiffness per cross-bridge of a muscle if all the azimuthal locations do not behave similarly.

Variation in the behavior of cross-bridges depending upon the azimuthal location of the actin site, as seen in Tables I–III, is model-dependent. Models very similar to the ones reported here, but for which the cross-bridges attach to actin slewed, (for example, $\gamma = 90°$ instead of 0°) show very little variation in cross-bridge behavior with actin site azimuthal location, even over the entire range, $\phi = 0$–$120°$ (unpublished computations). This difference between models results because, when $\gamma = 90°$, the location of the S1–S2 junction in space does not vary so greatly with changes of actin site azimuthal angle as it does when $\gamma = 0°$. It should be noted that the three-dimensional reconstruction of Moore et al. (1970) shows the S1 head appearing to attach to actin along its side, more like the case $\gamma = 90°$.

Because of the difference in behavior of cross-bridges at different actin site locations, some of the conclusions drawn concerning Models I–III were only borderline true for $\phi = 120°$. This is probably not significant, since cross-bridges may be required to attach to actin sites located over an azimuthal range of only 90° (Squire, 1972; Haselgrove and Reedy, 1978).

In summary, three models of cross-bridge geometry have been examined. By using parameter values consistent with those currently thought most appropriate (long S2, γ similar to 90°), these models produce approximately constant axial force at different filament separations. However, we have illustrated that several factors affecting cross-bridge distribution or geometry can cause deviations from this behavior.

APPENDIX I

Transformation between Variables in Different Reference Frames

The equations describing the cross-bridge are more compactly written and derived using variables referenced to plane *DFBG* (Fig. 1), namely Z' ($= \overline{DF}$) and δ, rather than the more commonly referred to variables, Z (filament separation) and ϕ (azimuthal angle), which derive from the plane of the filament axes. The two sets of variables are related as follows. Z' may be found by dropping a perpendicular from F to OO' (Fig. 1 *B*) and from D to the first perpendicular. The intersection of the two perpendiculars is point H. Since $\overline{OD} = \ell_A$ and $\overline{O'F} = \ell_B$, it may be readily shown that

$$\begin{aligned}\overline{FH} &= \overline{O'F}\sin\theta - \overline{OD}\sin\phi \\ &= \ell_M \sin\theta - \ell_A \sin\phi\end{aligned}$$

and

$$\begin{aligned}\overline{DH} &= \ell_A + Z + \ell_M - \overline{OD}\cos\phi - \overline{O'F}\cos\theta \\ &= \ell_A + Z + \ell_M - \ell_A\cos\phi - \ell_M\cos\theta.\end{aligned}$$

By Pythagorus' theorem

$$Z' = \overline{DF} = (\overline{FH}^2 + \overline{DH}^2)^{1/2}. \tag{A1.1}$$

Since the angle that DF makes with OO', ϵ, may be found from $\epsilon = \tan^{-1}(\overline{FH}/\overline{DH})$, then, from Fig. 1 *B*, the angle, δ, is simply

$$\delta = \phi - \gamma - \epsilon. \tag{A1.2}$$

APPENDIX II

Calculation of the Torque about ∠ACD due to the Force (F) in AB

The torque about $\angle ACD$ generated by the force, F, in the S2 link, AB in Fig. 1, can be calculated by calculating the component of F in plane ACD. How this is done can best be seen by viewing plane ACD from above, as shown in Fig. 6. We drop a perpendicular from point B on the myosin filament to plane ACD, and call the intersection of the perpendicular and the plane point J. The projection of the force, F, in AB is along AJ and has a magnitude $F\cos\angle BAJ = F \cdot \overline{AJ}/\ell_2$. This is the only component of the force in AB capable of producing a torque about C in plane ACD. The magnitude of that torque, τ, by the definition of torque, is $[(F \cdot \overline{AJ})/\ell_2] \cdot \ell_1 \cdot \sin\angle JAC$. Defining ζ as the angle that AJ makes with CD, dropping a perpendicular from J that intersects CD at K, and one from A that intersects JK at M (Fig. 6 *B*), we have $\angle JAM = \zeta$ and

$$\begin{aligned}\tau &= [(F \cdot \overline{AJ})/\ell_2] \cdot \ell_1 \cdot \sin(\alpha + \zeta) \\ &= [(F \cdot \overline{AJ})/\ell_2] \cdot \ell_1 \cdot (\cos\zeta\sin\alpha + \sin\zeta\cos\alpha).\end{aligned}$$

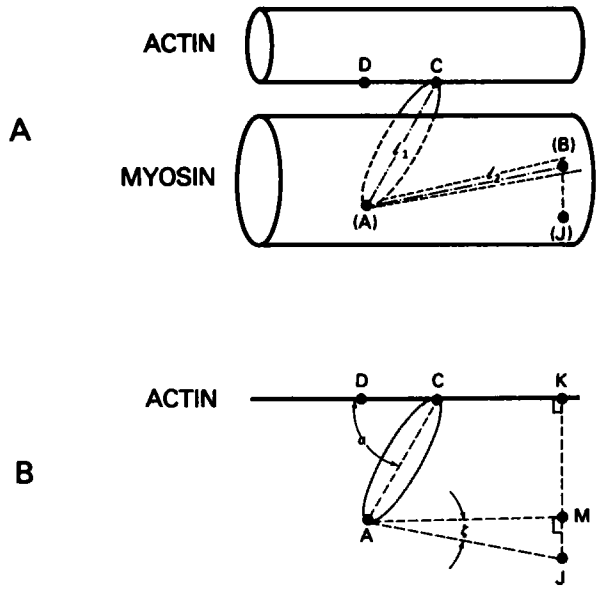

FIGURE 6 (*A*) Cross-bridge and filaments as seen looking down upon the plane (*ACD*) determined by the S1 head and line *DCG* of Fig. 1 *A*. The myosin filament in this instance is above plane *ACD*. A perpendicular from the S2-myosin backbone junction, *B*, intersects plane *ACD* at *J*. (*B* is on the undersurface of the myosin filament here.) (*B*) Identical view of plane *ACD* with filaments and S2 not shown.

From Figs. 1 *B* and 6 *B*

$$\sin \zeta = (\overline{JK} - \overline{MK})/\overline{AJ}$$
$$= (Z' \cos \delta - \ell_1 \sin \alpha)/\overline{AJ}$$

and

$$\cos \zeta = \overline{AM}/\overline{AJ}$$
$$= (x + \ell_1 \cos \alpha)/\overline{AJ}$$

so that

$$\tau = F \cdot \ell_1 [(x + \ell_1 \cos \alpha) \sin \alpha + (Z' \cos \delta - \ell_1 \sin \alpha) \cos \alpha]/\ell_2$$
$$= F \cdot \ell_1 [x \sin \alpha + Z' \cos \delta \cos \alpha)/\ell_2. \quad \text{(A2.1)}$$

APPENDIX III

Relating the Length of S2, ℓ_2, to Other Geometric Variables

Considering $\triangle ADF$ and $\triangle ACD$ in Fig. 1 *A*, we have $\angle ACD \equiv \alpha$, $\angle ADC = 90°$, so that $\overline{AD} = \overline{AC} \sin \alpha \equiv \ell_1 \sin \alpha$. Knowing two sides and an included angle in $\triangle ADF$, one may find the opposite side, $\overline{AF}$, according to

$$\overline{AF} = [(\overline{AD})^2 + (\overline{DF})^2 - 2(\overline{AD})(\overline{DF}) \cos \angle ADF]^{1/2}$$
$$= [(\ell_1 \sin \alpha)^2 + Z'^2 - 2Z'\ell_1 \sin \alpha \cos \delta]^{1/2}, \quad \text{(A3.1)}$$

where Z' has been written for $\overline{DF}$ and δ for $\angle ADF$. Considering $\triangle ABF$; $\overline{EB} \equiv x$ and $\overline{FE} = \overline{DC}$ and from $\triangle ADC$, $\overline{DC} = \ell_1 \cos \alpha$, so that

$$\overline{FE} = \ell_1 \cos \alpha$$

and

$$\overline{FB} = \overline{FE} + \overline{EB} = \ell_1 \cos \alpha + x. \tag{A3.2}$$

Since $\overline{AB} = [(\overline{AF})^2 + (\overline{FB})^2]^{1/2}$, we have, substituting from Eqs. A3.1 and A3.2

$$\ell_2 \equiv \overline{AB} = [(\ell_1 \sin \alpha)^2 + Z'^2 - 2Z'\ell_1 \sin \alpha \cos \delta + (x + \ell_1 \cos \alpha)^2]^{1/2},$$

which simplifies to

$$\ell_2 = [Z'^2 + \ell_1^2 + x^2 + 2\ell_1 (x \cos \alpha - Z' \cos \delta \sin \alpha)]^{1/2}. \tag{A3.3}$$

Received for publication 21 May 1979 and in revised form 25 October 1979.

REFERENCES

BURKE, M., S. HIMMELFARB, and W. F. HARRINGTON. 1973. Studies on the "hinge" region of myosin. *Biochemistry.* **12:** 701–710.

EISENBERG, E., and T. L. HILL. 1978. A cross-bridge model of muscle contraction. *Prog. Biophys. Mol. Biol.* **33:** 55–82.

ELLIOTT, A., and G. OFFER. 1978. Shape and flexibility of the myosin molecule. *J. Mol. Biol.* **123:** 505–519.

ELLIOTT, G. F., J. LOWY, and B. MILLMAN. 1967. Low angle x-ray diffraction studies of living striated muscle during contraction. *J. Mol. Biol.* **25:** 31–45.

FORD, L. E., A. F. HUXLEY, and R. M. SIMMONS 1977. Tension responses to sudden length change in stimulated frog muscle fibres near slack length. *J. Physiol. (Lond.).* **269:** 441–515.

GODT, R. E., and D. W. MAUGHAM 1977. Swelling of skinned muscle fibers of the frog. *Biophys. J.* **19:** 103–116.

GOLDMAN, Y. E., and R. M. SIMMONS 1978. Stiffness measurements on frog skinned muscle fibers at varying interfilamentary separation. *Biophys. J.* **21:** 86*a*. (Abstr.)

GOODY, R. S., K. C. HOLMES, H. G. MANNHERZ, J. BARRINGTON LEIGH, and G. ROSENBAUM. 1975. Cross-bridge conformation as revealed by x-ray diffraction studies with ATP analogues. *Biophys. J.* **15:**687–705.

GORDON, A. M., A. F. HUXLEY, and F. J. JULIAN. 1966. The variation in isometric tension with sarcomere length in vertebrate muscle fibres. *J. Physiol. (Lond.).* **184:**170–192.

HASELGROVE, J. C., and M. K. REEDY. 1978. Modeling rigor cross-bridge patterns in muscle. I. Initial studies of the rigor lattice of insect flight muscle. *Biophys. J.* **24:**713–728.

HILL, T. L. 1970. Sliding filament model of muscular contraction. V. Isometric force and interfilament spacing. *J. Theor. Biol.* **29:**395–410.

HILL, T. L. 1974. Theoretical formalism for the sliding filament model of contraction of striated muscle. Part I. *Prog. Biophys. Mol. Biol.* **28:**267–340.

HILL, T. L. 1975. Theoretical formalism for the sliding filament model of contraction of striated muscle. Part II. *Prog. Biophys. Mol. Biol.* **29:**105–159.

HUXLEY, A. F. 1957. Muscle structure and theories of contraction. *Prog. Biophys. Biophys. Chem.* **7:**255–318.

HUXLEY, A. F., and R. M. SIMMONS. 1971. Proposed mechanism of force generation in striated muscle. *Nature (Lond.).* **233:**533–538.

HUXLEY, H. E. 1963. Electron microscopic studies on the structure of natural and synthetic protein filaments from skeletal muscle. *J. Mol. Biol.* **71:**281–308.

HUXLEY, H. E. 1969. The mechanism of muscular contraction. *Science (Wash. D.C.)* **164:**1356–1366.

HUXLEY, H. E., and W. BROWN. 1967. The low-angle x-ray diagram of vertebrate striated muscle and its behaviour during contraction and rigor. *J. Mol. Biol.* **30:**383–434.

LOWEY, S., H. S. SLAYTER, A. WEEDS, and H. BAKER. 1969. Structure of the myosin molecule. II. Subfragments of myosin by enzymic degradation. *J. Mol. Biol.* **42:**1–29.

MARSTON, S. B., C. D. RODGER, and R. T. TREGEAR. 1976. Changes in muscle crossbridges when β,γ-imido-ATP binds to myosin. *J. Mol. Biol.* **104**:263–276.

MARSTON, S. B., R. T. TREGEAR, C. D. RODGER, and M. L. CARKE. 1979. Coupling between the enzymatic site of myosin and the mechanical output of muscle. *J. Mol. Biol.* **128**:111–126.

MENDELSON, R. A., M. F. MORALES, and J. BOTTS. 1973. Segmental flexibility of the S-1 moiety of myosin. *Biochemistry.* **12**:2250–2255.

MOORE, P. B., H. E. HUXLEY, and D. J. DEROSIER. 1970. Three-dimensional reconstruction of F-actin, thin filaments and decorated thin filaments. *J. Mol. Biol.* **50**:279–295.

REEDY, M. K. 1967. Cross-bridges and periods in insect flight muscle. *Am. Zool.* **7**:465–481.

REEDY, M. K., K. C. HOLMES, and R. T. TREGEAR. 1965. Induced changes in orientation of the cross-bridges of glycerinated insect flight muscle. Nature *(Lond.)* **207**:1276–1280.

SQUIRE, J. M. 1972. General model of myosin filament structure. II. Myosin filaments and cross-bridge interactions in vertebrate striated and insect flight muscles. *J. Mol. Biol.* **72**:125–138.

SQUIRE, J. M. 1975. Muscle filament structure and muscle contraction. *Annu. Rev. Biophys. Bioeng.* **4**:137–161.

SUTOH, K., Y-C. C. CHIAO, and W. F. HARRINGTON. 1978. Effect of pH on cross-bridge arrangement on synthetic myosin filaments. Biochemistry. **17**:1234–1239.

TER KEURS, H. E. D. J., T. IWAZUMI, and G. H. POLLACK. 1978. The sarcomere length-tension relation in skeletal muscle. *J. Gen. Physiol.* **72**:565–592.

WRAY, J. S., P. J. VIBERT, and C. COHEN. 1975. Diversity of cross-bridge configurations in invertebrate muscles. *Nature (Lond.).* **257**:561–564.